Insight towards the role of platinum in the photocatalytic mineralisation of organic compounds

Frans Denny, Jason Scott, Ken Chiang, Wey Yang Teoh, Rose Amal[*]

ARC Centre for Functional Nanomaterials, School of Chemical Sciences and Engineering, The University of New South Wales, Sydney, NSW 2052, Australia

Abstract

The mineralisation of functionalised (hydroxyl and carboxylic) organic compounds by platinum deposits on titanium dioxide (Pt/TiO$_2$) was investigated to study the catalytic and photocatalytic roles of platinum and the effect of organic molecular structure on these properties. Under dark conditions Pt/TiO$_2$ catalysed the complete mineralisation of formic acid and partial mineralisation of oxalic acid and 1,2,3-trihydroxybenzene (1,2,3-THB). Under irradiated conditions, platinum deposits improved the mineralisation rate of each organic considered. Increasing carbon chain length of aliphatic compounds decreased mineralisation rates by both bare TiO$_2$ and Pt/TiO$_2$, attributed to steric hindrance effects for alcohols and the formation of rate limiting intermediates for carboxylic acids. Increasing the number of hydroxyl groups in aliphatic compounds increased mineralisation rates only by Pt/TiO$_2$. This effect was not evident for hydroxylated aromatics. The findings suggest the degree of catalysis invoked by platinum deposits during photocatalysis is governed by the structural and functional characteristics of the target organic.
© 2006 Published by Elsevier B.V.

Keywords: Platinum; Titanium dioxide; Photocatalysis; Photodeposition

1. Introduction

Metal deposition on TiO$_2$ has been intensively studied as a means of reducing electron/hole recombination and enhancing photocatalytic efficiencies. Metals typically deposited on TiO$_2$ are transition or noble metals such as iron (Fe) [1], silver (Ag) [1,2] or platinum (Pt) [3–9]. Pt is of particular interest as it displays a high work potential, allowing it to trap a large number of electrons [10]. When Pt is photodeposited onto the surface of TiO$_2$ a Schottky junction at the metal–TiO$_2$ interface develops resulting in the movement of electrons from the conduction band of TiO$_2$ to the metal, consequently trapping electrons at the metal surface [11]. Trapping these electrons inhibits electron/hole recombination, providing more efficient charge separation. Pt also possesses hydro-

genation, dehydrogenation and oxidation capabilities in thermal catalysis, which may also prove beneficial during photocatalysis.

Pt deposited on TiO$_2$ has been reported to improve [3–9,12–17], be detrimental [5,16] or have negligible effects [6] on photocatalysis. Vorontsov and Dubovitskaya [12] reported up to a two times increase in the rate of ethanol photooxidation at various Pt loadings and He et al. [14] reported a 4.2 times rate increase when photocatalytically degrading formic acid using photodeposited Pt (0.64 at.% loading) on a sol–gel coated TiO$_2$ thin film. Chen et al. [16] observed a 2.5 times decrease in the chloroform degradation rate and a 12 times decrease in the degradation of trichloroethylene for 1 at.% Pt on Degussa P25 TiO$_2$. Coleman et al. [6] found 2 at.% platinised Degussa P25 exhibited no effects when degrading selected endocrine disrupting chemicals although the low concentrations of organics required to mimic environmental levels meant the conditions were in the mass transfer limited domain. Lee and Choi [15] found the effects of TiO$_2$ platinisation depend on the oxidation state of Pt and type of substrate being degraded. They reported Pt^0 as the most active oxidation state of the Pt deposits for the organic substrates they considered.

* Corresponding author at: School of Chemical Sciences and Engineering, Applied Science Building, The University of New South Wales, Sydney, NSW 2052, Australia. Tel.: +61 2 9385 4361; fax: +61 2 9385 5966.
E-mail addresses: frans@student.unsw.edu.au (F. Denny), jason.scott@unsw.edu.au (J. Scott), k.chiang@unsw.edu.au (K. Chiang), wy.teoh@student.unsw.edu.au (W.Y. Teoh), r.amal@unsw.edu.au (R. Amal).

The choice of target organic may also govern the performance of Pt/TiO$_2$. Chen et al. [16] reported enhancement factors of three and two times for methanol and ethanol oxidation, respectively, by 1 at.% Pt photodeposited on Degussa P25. Moreover, this same photocatalyst displayed detrimental effects for the oxidation of chloroform and trichloroethylene. Hufschmidt et al. [8] observed a 2.6 times increase in the initial photonic efficiency of dichloroacetic acid degradation over 0.16 at.% Pt on Degussa P25, while a 1.5 times decrease was observed for 4-chlorophenol degradation.

While significant research has been devoted to the study of Pt/TiO$_2$ as a photocatalyst, many studies usually consider a limited number of target organics with particle characteristics or reaction conditions being varied in preference. Very few studies have systematically examined the influence of organic molecular structure on the effects provided by Pt deposition on TiO$_2$ as a means of understanding the actions of Pt in photodegradation. This paper presents work on the influence of molecular structure and number and type of functional groups (hydroxyl and carboxylic) on the photocatalytic mineralisation by bare or platinised TiO$_2$ and considers whether Pt deposits invoke beneficial effects beyond simply an improvement in electron/hole separation. The catalytic effect of Pt deposits on selected organics is also investigated.

2. Experimental

2.1. Chemicals

Degussa P25, comprising non-porous particles with an anatase to rutile ratio of 3:1 [18] was the source of TiO$_2$. Hexachloroplatinic acid (Aldrich, 99%) was used as the precursor for platinum deposition. Perchloric acid (Unilab, 99%), required for pH control, was used as supplied. Eighteen organics were selected for this work based on their molecular structure (linear or aromatic) and the type and number of hydroxyl and/or carboxylic functional groups. Each molecule can be classed in one of four groups: (1) mono-carboxylic acids—formic acid (Ajax, 98%), acetic acid (Ajax, 99.7%), propanoic acid (Sigma–Aldrich, 99%) and butyric acid (Aldrich, >99%); (2) dicarboxylic acids—oxalic acid (Unilab, anhydrous), malonic acid (Sigma–Aldrich, 99%), succinic acid (Sigma–Aldrich, >99%), malic acid (Sigma, >99%) and tartaric acid (Aldrich, 99%); (3) alcohols and diols—methanol (Unilab, anhydrous), ethanol (Aldrich, absolute), ethane-diol (Ajax APS, 100%), propan-1-ol (BDH, 99%), propane-1,2-diol (Quest, 99%) and propane-triol (Sigma, 99%); (4) aromatics—phenol (BDH, 99%), resorcinol (Unilab, 100%) and 1,2,3-trihydroxybenzene (1,2,3-THB (Sigma–Aldrich, 100%)) All organics were used as supplied and all solutions were prepared using deionised water (Millipore Milli-Q).

2.2. Pt/TiO$_2$ preparation and characterisation

An annular photoreactor, as described by Chiang et al. [3], was utilised for the preparation of Pt/TiO$_2$. A pre-determined volume of 1 g/L TiO$_2$ slurry was sonicated for 15 min before

being charged to the photoreactor upon which it was UV-irradiated for 30 min to remove adsorbed organic impurities. Pt precursor, at a 0.5 at.% loading on TiO$_2$, and methanol, to act as a hole scavenger during the photoreduction process, were added. The Pt loading was selected according to the findings of Teoh et al. [13] who had previously determined this loading as the optimum for sucrose mineralisation. Suspension pH was adjusted to 3.00 ± 0.05 by perchloric acid addition and the solution circulated for 20 min to allow for dark adsorption of the organics. Over the final 10 min of dark adsorption the suspension was purged with nitrogen gas at 50 mL/min and continued during photodeposition to provide anoxic conditions. The target organic was mineralised by irradiating the slurry for 1 h. An NEC T10 blacklight blue (20 W) lamp provided the source of UV-A light. The Pt/TiO$_2$ particles were recovered by centrifugation (Beckmann Coulter Allegra 25R Centrifuge) at 10,000 rpm for 10 min and washed four times to remove residual chloride ions remaining from the platinum precursor. The washed particles were dried in an oven at 60 °C and stored in a desiccator prior to use. The BET surface areas of TiO$_2$ and Pt/TiO$_2$ were determined on a Micromeritics Tristar 3000. Transmission electron microscope (TEM) images were recorded by a Phillips CM200 TEM to confirm the presence of Pt deposits and give an indication of their size.

2.3. Dark adsorption of organics

Dark adsorption experiments were performed on both TiO$_2$ and Pt/TiO$_2$. Formic acid, oxalic acid and 1,2,3-THB adsorption results could only be attained for bare TiO$_2$ as these compounds underwent mineralisation by Pt/TiO$_2$ in dark conditions. Dark adsorption involved preparing a solution comprising 2000 μg carbon of an organic in 50 mL of 1 g/L photocatalyst suspension (pH adjusted to 3.00 ± 0.05) and agitating for 20 min. The mixture was filtered through a 0.2 μm PTFE membrane (Sartorius) and the filtrate analysed for total organic carbon (TOC) content by a Shimadzu TOC-V CSH Analyser.

2.4. Photocatalytic activity

Photocatalytic activities of the catalysts were assessed in a 50 mL slurry spiral photoreactor as described by Abdullah et al. [19]. A 1 g/L photocatalyst suspension was sonicated for 15 min and the pH adjusted to 3.00 ± 0.05 with perchloric acid. Adsorbed organic impurities on the catalyst surface were removed by irradiating the suspension in the spiral reactor for 30 min. The UV-A source was the same as that used for preparing the Pt/TiO$_2$ particles. The system was air equilibrated and 100 μL of solution, containing 2000 μg carbon in the form of the organic, added to the suspension. Dark adsorption of the organic on the TiO$_2$ was undertaken for 20 min whereby the suspension was irradiated. The suspension pH was not adjusted during the course of the reaction. The reaction kinetics were monitored by detecting CO$_2$ generation (mineralisation) via conductivity measurements.

The catalytic properties of Pt/TiO$_2$ for mineralising each organic were investigated by following the above experimental

procedure but without UV irradiation. Mineralisation was followed by analysing both CO_2 generation during, and TOC content at the end of, the reaction. Only formic acid, oxalic acid and 1,2,3-THB were found to undergo mineralisation by Pt/TiO_2 under dark conditions.

3. Results and discussion

The specific surface areas of TiO_2 and Pt/TiO_2 were determined as 51 (± 1) m^2/g and 49 (± 1) m^2/g, respectively, indicating platinisation provided no significant change in surface area. Iliev et al. [20] has similarly reported platinisation by photoreduction did not alter the surface area of Degussa P25. This finding reveals differences in the photoactivities of bare TiO_2 and Pt/TiO_2 are not due to surface area effects.

TEM (Fig. 1) confirmed the presence of Pt deposits on the surface of Degussa P25. Pt deposits are present on many of the TiO_2 particles in Fig. 1 and have diameters predominantly within the range 2.8 ± 0.6 nm (sample size ~20 Pt deposits).

3.1. Dark adsorption

Fig. 2 illustrates the degree of adsorption of each organic, in terms of carbon, on TiO_2 and Pt/TiO_2. The alcohols and poly-alcohols are the least adsorbed on TiO_2 and Pt/TiO_2. No evidence of methanol, ethanol or propane-1,2-diol adsorption is observed and the registered values for the other alcohols are either close to or below the lower limit of sensitivity of the instrument. This indicates the alcohols are poorly adsorbed on the surface of TiO_2 at room temperature, agreeing with reports by Tran et al. [2] and Diebold [21]. It is also apparent from Fig. 2 the Pt deposits have no significant effect on the extent of alcohol adsorption although Arévalo et al. [22] and Panja et al. [23] have indicated alcohols are capable of adsorbing on Pt metal. In this work, evidence of increased alcohol adsorption due to the Pt deposits may be hidden by the limited sensitivity of the analysis technique.
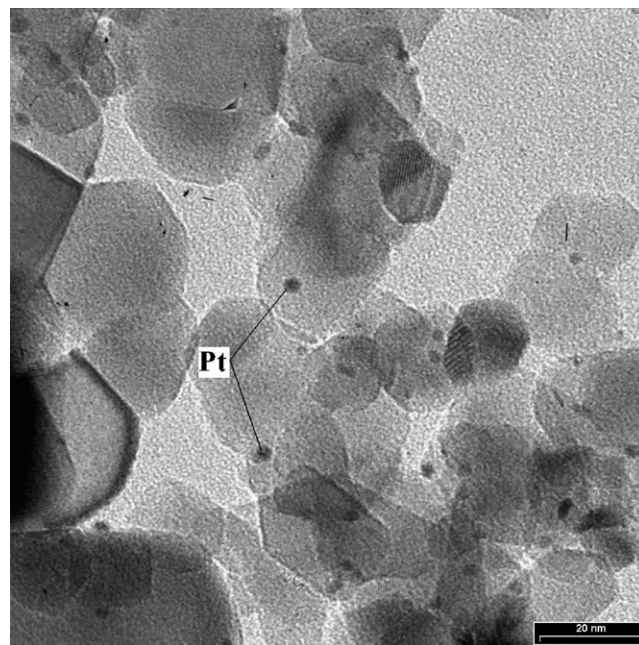

Fig. 1. TEM image of 0.5 at.% Pt/TiO_2 prepared by photodeposition on Degussa P25. Scale bar 20 nm.

With the exception of butyric acid, the carboxylic acids and di-carboxylic acids each adsorb on TiO_2 and Pt/TiO_2. Other workers [21] have reported carboxylic acids to be adsorbed on the surface of TiO_2. Fig. 2 also suggests Pt deposits increase adsorption of the carboxylic and di-carboxylic acids to different extents.

Fig. 2 indicates phenol does not adsorb on the surface of TiO_2, which is in agreement with Nagaveni et al. [24] who found that while phenol adsorbed on Degussa P25 after 30 h, over the first 2–3 h its adsorption was not appreciable. The results also suggest Pt deposits enhance phenol adsorption which agrees with findings by others [25,26] who have reported the adsorption of phenol on Pt surfaces. Fig. 2 also shows resorcinol, and to
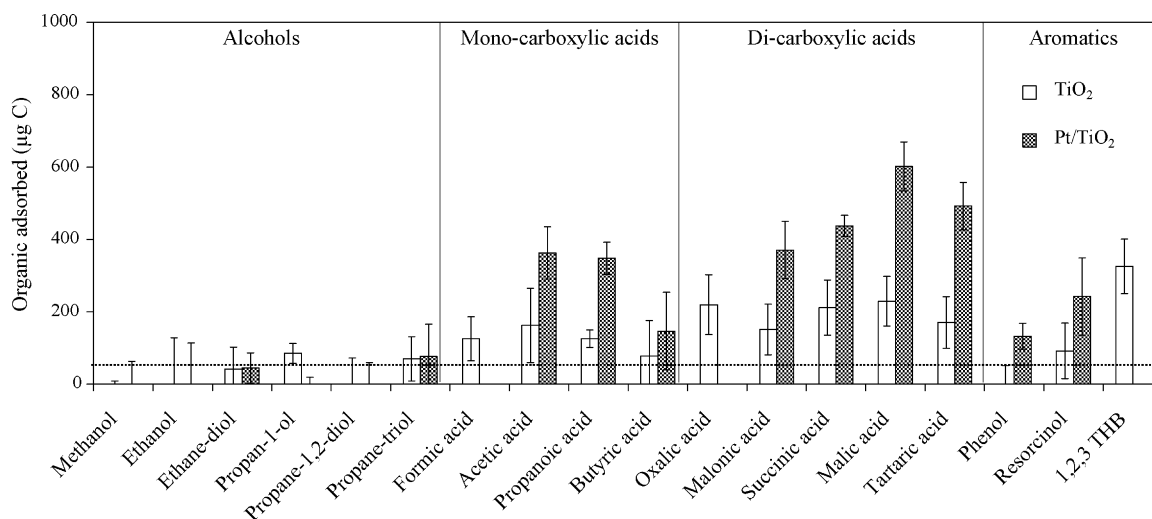

Fig. 2. Dark adsorption of selected organics onto TiO_2 and 0.5 at.% Pt/TiO_2. Catalyst loading 1 g/L; initial carbon concentration 2000 μg; adsorption period 20 min; initial pH 3.0. *Note*. lower limit of sensitivity of TOC analyser (50 μg C) included in figure.

a greater extent 1,2,3-THB, adsorb on TiO_2. The presence of Pt also appears to enhance the adsorption of resorcinol. Other work in our group (submitted for publication) found 1,2,3-THB to be readily adsorbed on Degussa P25 but found no evidence of resorcinol adsorption in the presence of either bare TiO_2 or Pt/TiO_2.

3.2. Catalytic effect of Pt/TiO_2

Under dark conditions and in the presence of Pt/TiO_2, CO_2 generation was observed for formic acid, oxalic acid or 1,2,3-THB, as shown in Fig. 3(a) and (b). In the case of formic acid, under dark conditions complete mineralisation was evident, with the rate comparable to the irradiated system (Fig. 3(a)). The catalytic action of Pt/TiO_2 on formic acid degradation has also been reported by He et al. [14] who found, at an equivalent Pt loading, approximately 20% mineralisation of 6300 μg carbon in the form of formic acid using a Pt/TiO_2 thin film on an indium–tin oxide conductive glass plate. The dark catalysis

displayed by Pt/TiO_2 could potentially be via dehydrogenation, oxidative dehydrogenation or hydrolysis by the Pt deposits, with the favored mechanism being unclear at the moment. Other workers have shown the proclivity for formic acid to undergo dehydrogenation on metals such as unsupported gold [27] and oxidation on palladium supported on TiO_2 [28] to give CO_2.

Under irradiated conditions, the mineralisation of oxalic acid (Fig. 3(a)) is rapid with a maximum rate of approximately 1550 μg C/min. Under dark conditions oxalic acid mineralisation is substantially slower with rate of ~7 μg C/min over the first 10 min, gradually decreasing to ~3.5 μg C/min at 120 min (Fig. 3(b)). This implies, under irradiated conditions, the mineralisation of oxalic acid is predominantly photocatalytic although simultaneous dark catalysis may also occur. At 120 min, under dark conditions approximately 28% of the available carbon has been converted to CO_2.

Fig. 3 also indicates under dark conditions Pt/TiO_2 is not as effective for mineralising oxalic acid compared to formic acid. This difference in rates may be due to the carbon–carbon (C–C)
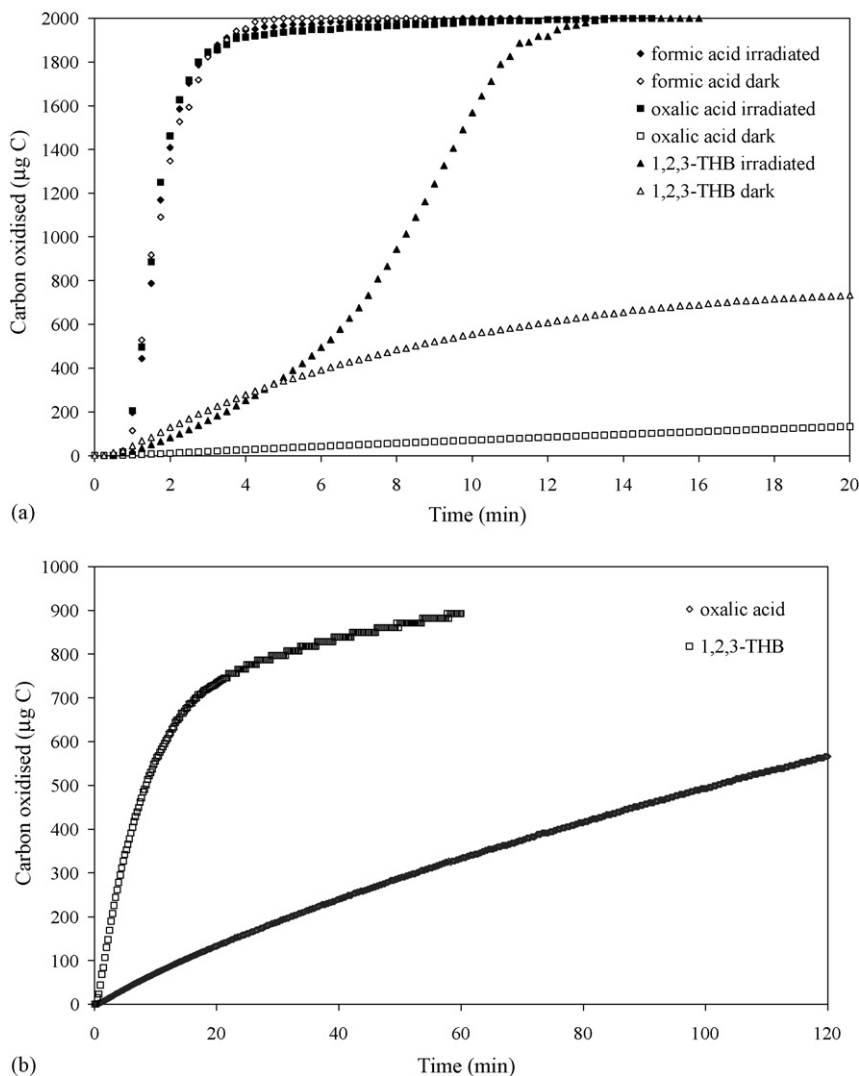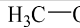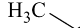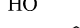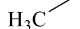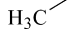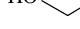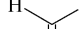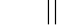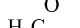

Fig. 3. Mineralisation profiles of: (a) formic acid, oxalic acid and 1,2,3-THB by 0.5 at.% Pt/TiO_2 in the presence and absence of UV irradiation and (b) oxalic acid and 1,2,3-THB by 0.5 at.% Pt/TiO_2 in the longer term. Catalyst loading 1 g/L; initial carbon loading 2000 μg C; initial pH 3.0.

bond in oxalic acid (Table 1) as Pt is not known for its ability to catalytically cleave C–C bonds [29]. Moreover, the ability of the Pt deposits to break the C–C bond in oxalic acid and not other di-carboxylic acids may be due to the two carbons in oxalic acid being components of carboxylic groups. The high electronegativities of the oxygen atoms in these groups may sufficiently weaken the C–C bond, allowing it to be cleaved by the Pt deposits. This effect is not evident in the longer-chain di-carboxylic acids due to a decrease in the chemical inductive effects of the carboxylic groups by the additional CH_2 groups.

Under irradiated conditions, 1,2,3-THB is initially miner- alised at a rate of ~70 μg C/min, whereby after approximately 5 min the rate accelerates to 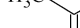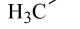reach a maximum of ~300 μg C/min at 7.5 min (Fig. 3(a)). The difference in CO_2 production rates during mineralisation implies the oxidation of a selected car- bon within the molecule dominates prior to oxidation of the next carbon. In this instance, the acceleration in rate occurs after approximately one-sixth of the total carbon available has formed CO_2. Given each 1,2,3-THB molecule contains six carbons, this suggests ring breakage and oxidation of the first carbon in the resulting straight chain dominates proceedings that is until this stage reaches completion. 1,2,3-THB is strongly adsorbed on the surface of TiO_2 [30] implying it adsorbs in preference to the generated intermediates (aldehydes and carboxylic acids [24]), restricting their access to the surface until the majority of the first carbon has been oxidised. Towards the end of this first step the intermediates will begin to access to the TiO_2 surface, the access increasing until all the 1,2,3-THB has been degraded whereby their degradation rates will dominate the result.

Under dark conditions, 1,2,3-THB mineralisation reaches an initial maximum rate of ~90 μg C/min after 2 min whereby the rate decreases to ~20 μg C/min after 15 min. The difference in the dark and irradiated profiles could be a function of the different reaction mechanisms driving the mineralisation. Under irradiated conditions, holes and hydroxyl radicals are continuously produced which are capable of completely oxi- dising 1,2,3-THB and its intermediates. Under dark conditions, the degradation mechanism is a function of the catalytic ability of Pt/TiO_2 which appears capable of initially oxidising carbons on compounds derived from the ruptured aromatic ring but finds it increasingly difficult to oxidise carbons in the resulting products. This is shown more clearly in the mineralisation of 1,2,3-THB over a longer time period (Fig. 3(b)). Here, two dis- tinct regimes exist in the mineralisation curve: (1) a higher rate of mineralisation of 1,2,3-THB over the first 15 min; (2) a lower rate of mineralisation of 1,2,3-THB from 15 min onwards. The 15 min point corresponds to around one-third of the available carbon having been mineralised, which can be interpreted as oxidation of two of the six carbons in each available aromatic ring. While the precise reaction mechanism is currently unclear, a possible reason for the two rate regimes may again lie with the influence of electronegativities and proximities of the oxygen molecules in the attached hydroxyl groups (see Table 1). In a similar manner to that discussed for oxalic acid, the oxygen atoms may weaken nearby C–C bonds in the aromatic ring (and subsequently in the straight-chain products) to an extent where they can be split by the action of Pt. As the carbons with

Table 1
Organic molecular structures and corresponding enhancement effects of Pt/TiO_2 over TiO_2

| Organic	Molecular structure	Enhancement effects
Methanol CH_4O		2.8
Ethanol C_2H_6O		2.5
Ethane-diol $C_2H_6O_2$		8.8
propan-1-ol C_3H_8O		2.2
Propane-1,2-diol $C_3H_8O_2$		3.3
Propane-triol $C_3H_8O_3$		8.9
Formic acid CH_2O_2		2.2
Acetic acid $C_2H_4O_2$		2.7
Propanoic acid $C_3H_6O_2$		2.4
Butyric acid $C_4H_8O_2$		1.9
Oxalic acid $C_2H_2O_4$		2.0
Malonic acid $C_3H_4O_4$		4.4
Succinic acid $C_4H_6O_4$		2.4
Malic acid $C_4H_6O_5$		6.3
Tartaric acid $C_4H_6O_6$		4.5
Phenol C_6H_6O		1.3
Resorcinol $C_6H_6O_2$		1.4
1,2,3-THB $C_6H_6O_3$		1.7
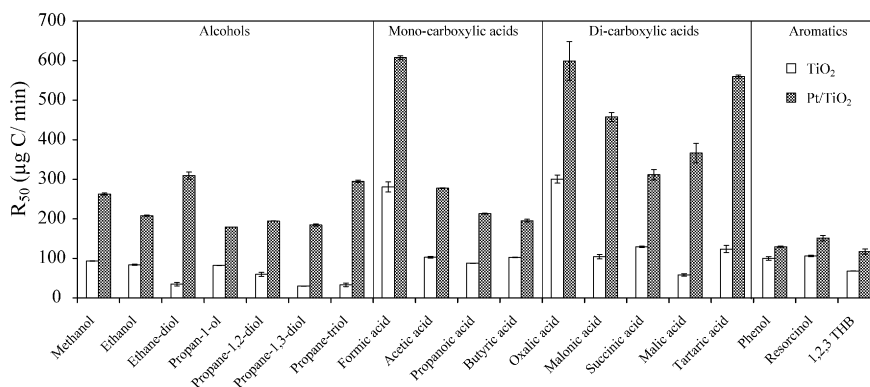
Fig. 4. Fifty percent mineralisation rates (R_{50}) of various organic compounds by TiO_2 and 0.5 at.% Pt/TiO_2. Catalyst loadings 1 g/L; initial carbon concentration 2000 µg; initial pH 3.0.

attached oxygen molecules are removed the remaining C–C bonds are less affected to a point where the Pt deposits find them difficult to rupture, leading to the decreased mineralisation rate. At this point in time, considerable uncertainty surrounds the implications of these results and studies are continuing to achieve a greater understanding of the role of Pt during dark mineralisation under ambient conditions.

3.3. Photocatalytic activities of TiO_2 and Pt/TiO_2

Fig. 4 depicts the 50% mineralisation rates (denoted by R_{50}) for the different classes of organic compounds degraded by TiO_2 and Pt/TiO_2. The 50% mineralisation rate is the (average) rate at which half the total organic carbon has been converted into carbon dioxide (CO_2). Values for the degree of enhancement imparted by the Pt deposits (ratio of R_{50} values) are provided in Table 1.

Fig. 4 shows in all cases Pt deposits enhance the mineralisation rates of the organics. The increase in R_{50} by Pt/TiO_2 for the mono- and di-carboxylic acids may be attributed to their adsorption on the photocatalyst, whereby they are susceptible to the increased hole availability invoked by the platinum deposits, although, as discussed later, other effects are also evident.

The alcohols do not extensively adsorb on the photocatalyst surface indicating that at least the parent molecules are not susceptible to the increased hole availability invoked by Pt. Intermediates generated during the degradation of the alcohol may adsorb on the photocatalyst surface and be subject to increased hole attack whereby, generally, alcohol degradation comprises a stage in the organic photodegradation cycle depicted in Fig. 5.
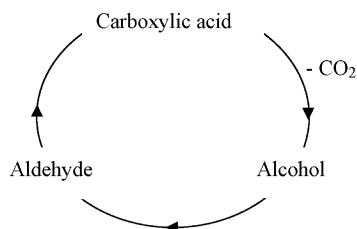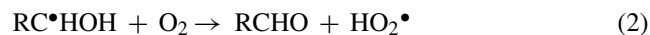

Fig. 5. Photodegradation cycle of simple carboxylic acids, alcohols and aldehydes.

The mechanism in each stage of the cycle involves:

1. The alcohol is attacked at the α-carbon by a hydroxyl radical (in solution) followed by oxygen to give an aldehyde via Eqs. (1) and (2) [31].

$$RCH_2OH + {}^\bullet OH \rightarrow RC^\bullet HOH + H_2O \tag{1}$$

$$RC^\bullet HOH + O_2 \rightarrow RCHO + HO_2{}^\bullet \tag{2}$$

Araña et al. [31] also suggest alcohols can dissociatively adsorb on the photocatalyst surface and undergo hole attack although given the negligible adsorption of alcohols portrayed in Fig. 2, it is thought hydroxyl attack in solution is more likely to occur.

2. Aldehydes can adsorb on the surface of TiO_2 [21] and assuming this is the case they react with two holes and a water molecule to give a carboxylic acid via Eq. (3) [32].

$$RCHO_{(ads)} + 2h^\bullet + H_2O \rightarrow RCOOH + 2H^+ \tag{3}$$
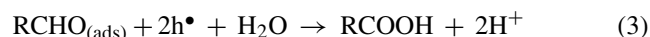
3. The carboxylic acid is adsorbed (dissociatively) on the TiO_2 surface [21] where it reacts with a hole (photo-Kolbe process) and hydroxyl radical to produce CO_2 and an alcohol via Eqs. (4) and (5).

$$RCOO_{(ads)}{}^- + h^\bullet \rightarrow R^\bullet + CO_2 \tag{4}$$

$$R^\bullet + {}^\bullet OH \rightarrow ROH \tag{5}$$
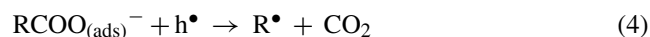
Ye et al. [33] have reported a similar degradation cycle to that described in Fig. 5 for the gas phase photocatalytic oxidation of aldehydes, except there was no indication alcohols were produced within their cycle. They indicated in the gas phase system pathways involving active oxygen species were more favoured than those involving hydroxyl groups. This is likely due to the limited presence of hydroxyl groups in the gas phase system and may explain the negligible presence of alcohol intermediates in their system.

It is also important to note in Fig. 5 and the accompanying equations that, given the nature of free radical chemistry, the cycle and mechanisms are not comprehensive in their assessment of all the possible reactions available, rather they provide

a simplified version of the reactions, which are expected to dominate during the degradation process. This point is illustrated in the work of Guillard et al. [34] who, while detecting aldehydes as the main product, also detected carboxylic acids, alcohols, alkanes and alkenes during the photocatalytic degradation of octanol.

The adsorption of aldehyde and carboxylic acid intermediates generated during alcohol degradation on the photocatalyst may explain the positive effect of the Pt deposits on alcohols. However, similar studies on alcohol mineralisation using silver (Ag) deposits on TiO_2 [2] demonstrated no positive effects of Ag despite Ag also being reported to improve electron/hole separation. The differences between the abilities of Ag and Pt to mineralise alcohols suggest factors, such as the catalytic ability of Pt, other than only improved electron/hole separation by the metal deposits are in effect.

Comparing the R_{50} values of singly hydroxylated alcohols for TiO_2 and Pt/TiO_2 in Fig. 4 shows they decrease in the order methanol > ethanol > propan-1-ol. Chen et al. [32,16] similarly reported higher methanol photooxidation and photomineralisation rates by Degussa P25 compared to ethanol. Moreover they found Pt deposition provided a three-fold increase in the mineralisation rate of methanol and a two-fold increase in the mineralisation rate of ethanol which are comparable to the values given in Table 1. Araña et al. [31] has also reported a lower photomineralisation rate for ethanol compared to methanol by Degussa P25 but found 1-propanol to possess a greater mineralisation rate than both these organics.

The observed decrease in rate with increasing carbon chain length may result from a number of factors including increased steric hindrance effects with increasing carbon number hindering hydroxyl radical attack on the hydroxylated carbon (particularly with the growth from one to two carbon chains) or dilution of the positive charge on the hydroxylated carbon induced by the attached oxygen atom, reducing the attraction between it and the attacking hydroxyl radical. Alternately, degradation of the aldehyde product may be governing the alcohol mineralisation rate.

Similarly, Fig. 4 shows adverse effects of additional CH_2 groups on R_{50} are observed for the mono-carboxylic acids (formic acid > acetic acid > propanoic acid > butyric acid). In this instance the decrease in R_{50} by the mono-carboxylic acids may be a result of the intermediates generated. According to the cycle in Fig. 5, butyric acid will degrade to form propan-1-ol, propanoic acid will degrade to form ethanol and acetic acid will degrade to form methanol. The R_{50} values for these pairs (Table 2) are comparable suggesting alcohol (or subsequent aldehyde) degradation may be rate limiting in the carboxylic acid degradation process.

Formic acid exhibits high R_{50} values, compared to the other carboxylic acids, as it is directly mineralised to CO_2 and H_2O with no alcohols or aldehydes formed as intermediates. Araña et al. [31] reported similar comparative effects for the photomineralisation of formic, acetic and propanoic acids.

The di-carboxylic acids also experience a decrease in R_{50} with increasing carbon chain length (oxalic acid > malonic acid > succinic acid). The significant decrease in R_{50} between oxalic and malonic acids shown in particular for TiO_2, is similar

Table 2
R_{50} values for carboxylic acids and alcohol pairs in the presence of TiO_2 and 0.5 at.% Pt/TiO_2

Carboxylic acid	R_{50} (μg C/min) TiO_2	Alcohol	R_{50} (μg C/min) TiO_2
Butyric acid	101	Propan-1-ol	82
Propanoic acid	88	Ethanol	84
Acetic acid	103	Methanol	94
Carboxylic acid	R_{50} (μg C/min) Pt/TiO_2	Alcohol	R_{50} (μg C/min) Pt/TiO_2
Butyric acid	197	Propan-1-ol	179
Propanoic acid	214	Ethanol	208
Acetic acid	278	Methanol	263

to the mono-carboxylic acid profiles suggesting an intermediate may be limiting the reaction rate for the longer chain acids. The increased complexity of the degradation mechanism evoked by the functional groups at each end of the di-carboxylic acid molecule has made it difficult to positively identify possible rate limiting intermediates at this time.

The effect of Pt deposits on the alcohol and mono-carboxylic acid R_{50} profiles depicted in Fig. 4 is predominantly to shift them to higher values and not alter their general shape, signifying the improvement is likely due to increased electron/hole separation. The R_{50} di-carboxylic acid profiles for TiO_2 and Pt/TiO_2 differ significantly, suggesting the role of Pt may extend beyond acting only to improve electron/hole separation in this instance.

The presence of additional hydroxyl groups in alcohol or di-carboxylic acid molecules appear to have an influence on the R_{50} value, particularly for the Pt/TiO_2 particles. Fig. 4 indicates additional OH groups on two-carbon alcohols (ethanol, ethanediol) and three-carbon alcohols (propan-1-ol, propane-1,2-diol, propane triol) are detrimental to R_{50} values for TiO_2 whereas they are beneficial for Pt/TiO_2.

To gain a greater understanding of the differences between mineralisation of the alcohols/polyols by bare and platinised TiO_2 their complete mineralisation curves are required. These are provided in Fig. 6(a) and (b), respectively. The mineralisation profiles for bare TiO_2 show ethanol and propan-1-ol curves to be similar and possess the highest rate, the ethane diol and propane triol curves to be similar and possess the lowest rate and the propane-1,2-diol curve to lie in between and possess two overlapping rate regimes. The first regime in the propane-1,2-diol curve has a rate similar to the other polyols with the second regime similar to that for the alcohols.

The differing mineralisation rates for bare TiO_2 are attributed to the number and location of the hydroxyl groups within each molecule as, given the initial step of alcohol mineralisation is via hydroxyl radical attack (Eq. (1)), the hydroxyl groups influence the ease by which the hydroxyl radicals can attack the molecule. That is, the hydroxylated end group of ethanol and propan-1-ol is more readily accessible by hydroxyl radicals than the end groups of ethane diol and propane triol as the hydroxyl groups on adjacent carbons in the polyols impede the radical attack. In the instance of propane-1,2-diol, initial hydroxyl radical attack is hindered by the hydroxyl group adjacent to the hydroxylated end
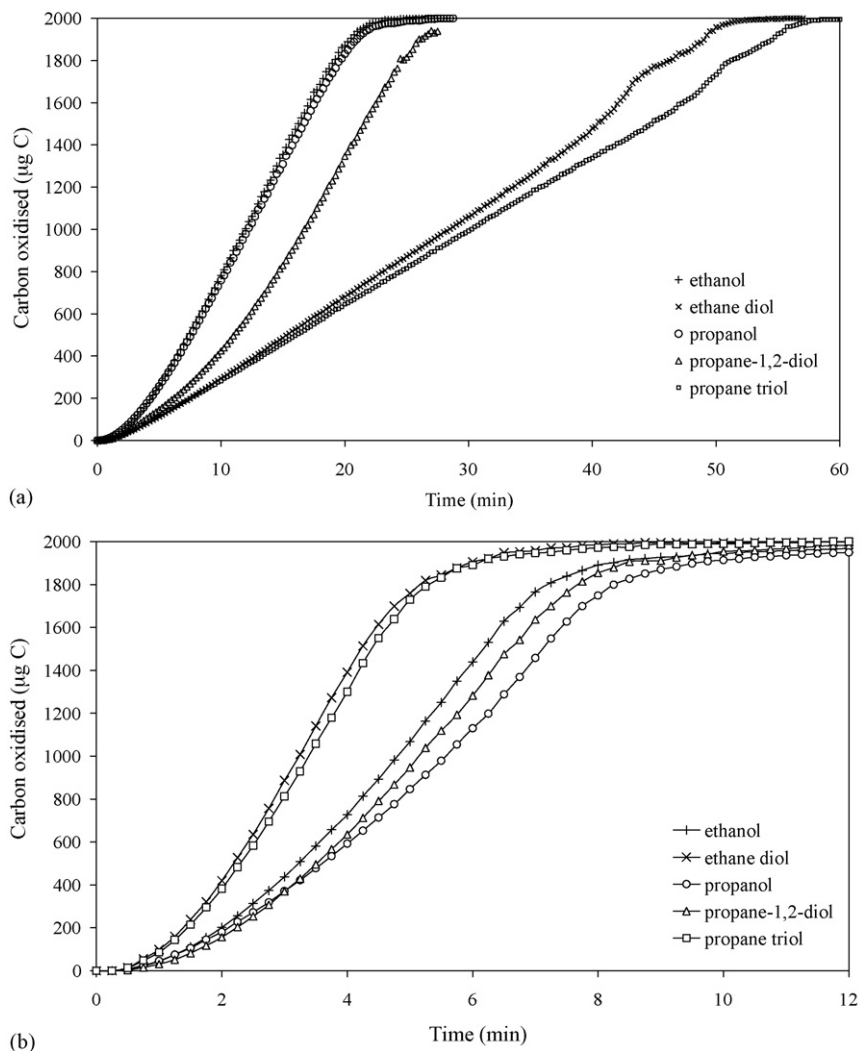
Fig. 6. Photocatalytic mineralisation curves for alcohols/polyols in the presence of (a) bare TiO_2 and (b) 0.5 at.% Pt/TiO_2. Initial carbon concentration 2000 μg; photocatalyst loading 1 g/L; pH 3.0.

group as shown by the lower mineralisation rate over approximately the first-third of total carbon mineralised in Fig. 6(a). However, according to the cycle in Fig. 5, the product following mineralisation of the first carbon in propane-1,2-diol will be acetaldehyde. Acetaldehyde is also formed during the mineralisation of ethanol and propanol and the similar rates of these two profiles to that of the latter stages of propane-1,2-diol support the formation of acetaldehyde as an intermediate during its degradation.

Pt deposits significantly alter the relative mineralisation rates of the alcohols/polyols whereby the rates for ethane diol and propane triol are themselves similar and greater than the similar rates of ethanol and propanol (Fig. 6(b)). Moreover, the mineralisation rate of propane-1,2-diol is comparable to ethanol and propanol, implying the hydroxyl group adjacent to the hydroxylated end carbon has little influence on the mineralisation process in the presence of Pt/TiO_2. If the initial degradation step of the alcohols/polyols remained hydroxyl radical attack in solution for Pt/TiO_2, given the mechanism proposed for bare TiO_2 it would be expected the relative mineralisation rates

would remain unchanged to those seen for bare TiO_2, that is ethanol ≈ propanol > propane-1,2-diol > ethane diol ≈ propane triol, but shifted to higher values. This would only occur if it was assumed the improved electron/hole separation invoked by Pt produced greater numbers of hydroxyl radicals and the availability of these radicals was the rate limiting step in the bare TiO_2 case. The variation in the rates order for Pt/TiO_2 suggests a different degradation process to that encountered for bare TiO_2 is in effect. If the degradation does not occur in solution, then the alternative is it occurs on the surface of the particles. For this to be the case the alcohols/polyols would need to adsorb on the photocatalyst, or more specifically on the Pt deposits. Fig. 2 does not indicate any additional adsorption of alcohols or polyols occurs on Pt/TiO_2 with reasons for this discussed earlier in Section 3.1. Literature [22,23] supports the idea of alcohol adsorption, indicating alcohols can adsorb on platinum and other noble metals and furthermore these metals are capable of catalysing the oxidative dehydrogenation of alcohols [35–37]. Yang et al. [37] proposed a mechanism for the silver-catalysed oxidative dehydrogenation of alcohols involving the injection of

two electrons by the silver into an adsorbed oxygen molecule, resulting in its cleavage to give two atomic oxygens, O^-. Each atomic oxygen then extracted two hydrogens from an adsorbed alcohol molecule to give an aldehyde and water as products. It is reasonable to extend this mechanism to Pt (and possibly other metals) in photocatalysis given its capacity for trapping electrons upon irradiation and mediating their transfer to adsorbed species, such as O_2. Moreover, Einaga et al. [38] has reported Pt deposits are capable of stabilising O^- and O_3^- species which have been formed on the surface of photo-irradiated Degussa P25. In further support of this postulation, our group observed predominantly metallic Pt sites to be formed during the photodeposition of Pt on Degussa P25 under acidic conditions (submitted for publication), whereby Mallat and Baiker [35] reported only the metallic surface sites are active for the described oxidative dehydrogenation reaction.

In the instance of the hydroxylated C_4 di-carboxylic acids (succinic acid, malic acid, tartaric acid (Fig. 4)), bare TiO_2 is not consistently influenced by the presence additional hydroxyl groups but with Pt/TiO_2 there is a distinct increase in R_{50} with an increasing number of hydroxyl groups. As the di-carboxylic acids adsorb on bare TiO_2 (Fig. 2) they are subsequently available to hole attack. If the role of Pt was solely to improve electron/hole separation then, as was discussed for the alcohols/polyols, it would be expected the increase in mineralisation rate for each compound to be uniform in each case, that is, the order of rates should not vary. The variation in rate order suggests a second factor, such as the catalytic properties of Pt towards oxidative dehydrogenation, may also be improving the mineralisation of these compounds by Pt/TiO_2.

Fig. 4 shows increasing the number of hydroxyl groups on the aromatic ring has no consistent effect on the R_{50} values for either bare TiO_2 or Pt/TiO_2, despite the greater adsorption of organics with a higher number of hydroxyl groups (Fig. 2) and the observed catalytic effect of Pt/TiO_2 on 1,2,3-THB (Fig. 3). The similar order of mineralisation rates, that is resorcinol > phenol > 1,2,3-THB, for both bare TiO_2 and Pt/TiO_2 suggests the platinum deposits predominantly act to improve electron/hole separation. The catalytic effect of Pt/TiO_2 on 1,2,3-THB may manifest itself in the greater relative improvement in R_{50} values compared to phenol and resorcinol, as seen in Table 1, but it does not appear sufficient to provide 1,2,3-THB with the greatest overall mineralisation rate in the presence of Pt/TiO_2.

The early degradation stages of aromatics differ from the cycle described in Fig. 5, whereby the mechanism is reported [24] to involve the substitution of hydroxyl groups into the benzene ring until ring cleavage occurs. This addition is thought to occur in solution to provide various aromatic intermediates containing multiple hydroxyl groups prior to their interaction with the photocatalyst surface. For example, the addition of a first hydroxyl group to phenol is favoured in the *ortho* or *para* positions, to give catechol or hydroquinone, respectively [30]. This issue makes it difficult to discern the effects of additional hydroxyl groups for the three hydroxylated aromatics studied. Further work on other poly-hydroxylated aromatics is required to gain a greater understanding of these effects.

4. Conclusions

The deposition of platinum on the surface of TiO_2 was observed to improve the photocatalytic mineralisation rates for straight chain and aromatic compounds containing carboxylic acid and/or hydroxyl groups. Under dark conditions Pt/TiO_2 catalysed the complete or partial mineralisation of formic acid, oxalic acid and 1,2,3-THB.

The presence of Pt deposits was beneficial for the mineralisation of each organic considered. Increasing the carbon chain length of the mono-carboxylic and di-carboxylic acids decreased the mineralisation rates on a comparative basis and was attributed to steric hindrance or charge dilution effects in the case of alcohols and generated intermediates in the case of the carboxylic acids. Increasing the number of hydroxyl groups in the straight chain organics improved the mineralisation rates for alcohols/polyols and C_4-di-carboxylic acids on a comparative basis, indicating the enhancement provided by the Pt deposits could not be solely attributed to increased electron/hole separation. It was suggested the catalytic ability of Pt for the oxidative dehydrogenation of organics containing hydroxyl groups may play a role. This effect was not evident for hydroxylated aromatics. These findings suggest the catalytic properties of Pt may influence the photomineralisation of organics, the extent being a function of the characteristics of the organic under consideration.

Acknowledgements

References

[1] J. Araña, O.G. Díaz, M.M. Saracho, J.M.D. Rodríguez, J.A.H. Melián, J.P. Peña, Appl. Catal. B 36 (2002) 113.
[2] H. Tran, J. Scott, K. Chiang, R. Amal, J. Photochem. Photobiol. A 183 (2006) 41.
[3] K. Chiang, T.M. Lim, L. Tsen, C.C. Lee, Appl. Catal. A 261 (2003) 225.
[4] M. Linder, J. Theurich, D.W. Bahnemann, Water Sci. Technol. 35 (4) (1997) 79.
[5] J.C. Crittenden, J. Liu, D.W. Hand, D.L. Perram, Water Res. 31 (3) (1997) 429.
[6] H.M. Coleman, K. Chiang, R. Amal, Chem. Eng. J. 113 (2005) 65.
[7] W. Zhao, C. Chen, X. Li, J. Zhao, H. Hidaka, N. Serpone, J. Phys. Chem. B 106 (2002) 5022.
[8] D. Hufschmidt, D. Bahnemann, J.J. Testa, C.A. Emilio, M.I. Litter, J. Photochem. Photobiol. A 148 (2002) 223.
[9] U. Siemon, D. Bahnemann, J.J. Testa, D. Rodríguez, M.I. Litter, N. Bruno, J. Photochem. Photobiol. A 148 (2002) 247.
[10] K. Kalyanasundaram, in: M. Grätzel (Ed.), Energy Resources Through Photochemistry and Catalysis, Academic Press Inc., London, 1983, pp. 217–260.
[11] R. Memming, Semiconductor Electrochemistry, Wiley–VCH, Germany, 2001, pp. 24–36.
[12] A.V. Vorontsov, V.P. Dubovitskaya, J. Catal. 221 (2004) 102.
[13] W.Y. Teoh, L. Mädler, D. Beydoun, S.E. Pratsinis, R. Amal, Chem. Eng. Sci. 60 (2005) 5852.
[14] C. He, Y. Xiong, X. Zhu, X. Li, Appl. Catal. A 275 (2004) 55.
[15] J. Lee, W. Choi, J. Phys. Chem. B 109 (2005) 7399.
[16] J. Chen, D.F. Ollis, W.H. Rulkens, H. Bruning, Water Res. 33 (3) (1999) 661.

[17] J. Chen, D.F. Ollis, W.H. Rulkens, H. Bruning, Water Res. 33 (3) (1999) 669.

[18] T. Ohno, K. Sarukawa, K. Tokieda, M. Matsumura, J. Catal. 203 (2001) 82.

[19] M. Abdullah, G.K.-C. Low, R.W. Matthews, J. Phys. Chem. 94 (1990) 6820.

[20] V. Iliev, D. Tomova, L. Bilyarska, A. Eliyas, L. Petrov, Appl. Catal. B 63 (2005) 266.

[21] U. Diebold, Surf. Sci. Rep. 48 (2003) 53.

[22] M.C. Arévalo, J.L. Rodríguez, A.M. Castro-Luna, E. Pastor, Electrochim. Acta 51 (2006) 5365.

[23] C. Panja, N. Saliba, B.E. Koel, Surf. Sci. 395 (1998) 248.

[24] K. Nagaveni, G. Sivalingam, M.S. Hegde, G. Madras, Environ. Sci. Technol. 38 (2004) 1600.

[25] F. Lu, G.N. Salaita, L. Laguren-Davidson, D.A. Stern, E. Weller, D.G. Frank, N. Batina, D.C. Zapien, N. Walton, A.T. Hubbard, Langmuir 4 (1988) 637.

[26] H. Ihm, J.M. White, J. Phys. Chem. B 104 (2000) 6202.

[27] M.A. Bhakta, H. Austin Taylor, J. Chem. Phys. 44 (3) (1966) 1264.

[28] B. Xie, Y. Xiong, R. Chen, J. Chen, P. Cai, Catal. Commun. 6 (2005) 699.

[29] A. Yee, S.J. Morrison, H. Idriss, Catal. Today 63 (2000) 327.

[30] A.M. Piero, J.A. Allyon, J. Peral, X. Domenech, Appl. Catal. B 30 (2001) 359.

[31] J. Araña, J.M. Doña Rodríguez, O. González Díaz, J.A. Herrera Melián, J. Pérez Peña, Appl. Surf. Sci., in press (2005).

[32] J. Chen, D. Ollis, W.H. Rulkens, H. Bruning, Water Res. 33 (5) (1999) 1173.

[33] X. Ye, D. Chen, J. Gossage, K. Li, J. Photochem. Photobiol. A 183 (2006) 35.

[34] C. Guillard, P. Theron, P. Pichat, C. Petrier, Water Res. 36 (2002) 4263.

[35] T. Mallat, A. Baiker, Catal. Today (1995) 143.

[36] A.P. Markusse, B.F.M. Kuster, J.C. Schouten, in: Proceedings of the 8th International Symposium Catalyst Deactivation 1999, Brugge, Stud. Surf. Sci. Catal. 126 (1999) 273.

[37] Z. Yang, J. Li, X. Yang, X. Xie, Y. Wu, J. Mol. Catal. A 241 (2005) 15.

[38] H. Einaga, A. Ogata, S. Futamara, T. Ibusuki, Chem. Phys. Lett. 338 (2001) 303.